nature communications

Article

https://doi.org/10.1038/s41467-024-55310-x

Generation of perthiyl radicals for the synthesis of unsymmetric disulfides

Received: 29 June 2024

Accepted: 5 December 2024

Published online: 02 January 2025

Check for updates

Fei Zhou[1,3], Xiaochun He[1,3], Mi Zhou[1], Na Li[2], Qingqing Wang[1], Xuemei Zhang[1] & Zhong Lian[1]

Unsymmetric disulfides are prevalent in natural products and are essential in medicinal chemistry and materials science, but their robust synthesis poses significant challenges. In this paper, we report an expeditous transition-metal-free methodology for synthesizing unsymmetric disulfides through the addition of perthiyl radicals to alkenes. This study marks the use of generating perthiyl radicals by reacting SO_2 with unactivated alkyl (pseudo)halides (Cl/Br/I/OTs). Various primary, secondary and tertiary alkyl (pseudo)halides substituted with different functional groups successfully function as suitable reactants. The formation of perthiyl radicals and their involvement in the reaction process are verified through mechanistic studies and DFT calculations. Overall, this method leverages readily available alkyl electrophiles and alkenes alongside SO_2 in a single reaction setup to efficiently form both carbon-sulfur and sulfur-sulfur bonds simultaneously.

Disulfides are widely utilized across various disciplines, including biology[1], food chemistry[2], and pharmaceutical sciences[3]. Of particular note is the pharmaceutical industry's effective employment of S-S bond linkers in formulating a range of therapeutics aimed at treating diabetes, alcoholism, and cancer, through their incorporation into antibody, small molecules and peptides (Fig. 1A)[4–8].

Traditional methods to prepare disulfides primarily rely on the disulfide exchange or the couplings of two sulfur-containing compounds. Contemporary strategies for disulfide synthesis often employ disulfurating reagent (RSS^-LG) to forge C-SS bonds, with persulfide cations (RSS^+) or persulfide anions (RSS^-) serving as crucial intermediates[9–21] (Fig. 1B). However, there have been no reports on a method for directly synthesizing unsymmetrical disulfides using perthiyl radicals (RSS•)[22–25]. To date, several methods have been explored for generating perthiyl radicals (Fig. 1B), and one of the earliest methods involved the thermal decomposition of tetrasulfides[26–29]. However, the reverse reaction, i.e., the dimerization of RSS•, occurs with minimal or no activation energy, resulting in low overall conversion[30]. An alternative approach involves carbon radical substitution on tetrasulfides[31,32]. Additionally, the hydrogen-atom-transfer (HAT) process emerges as a powerful and effective strategy for radical production, as the relatively weak RSS–H bond dissociation enthalpy (~70 kcal/mol) enables the oxidation of hydropersulfides to RSS• by mild oxidants[33–35]. Another potent and efficient strategy is photochemistry, which activates S-Cl bonds in RSSCl to form perthiyl radicals[26]. Unfortunately, these methods for generating perthiyl radicals often require stringent experimental conditions and can only be applied to the pre-synthesized polysulfides. Furthermore, the preparation of polysulfides is often complex and time-consuming. Hence, the development of a versatile and convenient approach for generating perthiyl radicals in a single reaction remains a significant priority. This will not only greatly simplify the process of preparing unsymmetric disulfides but also improve synthesis efficiency.

On the other hand, sulfur dioxide (SO_2) is widely used in the pharmaceutical and organic chemical synthesis sectors[36–66]. In recent years, our research group has focused on the versatile chemical properties of SO_2 and developed several synthetic methods in which are carbon radicals capture SO_2 molecule to form sulfonyl radicals. Building on our previous work involving sulfonyl radicals, the objective of this study is to develop a general approach using SO_2 as

[1]Department of Dermatology, State Key Laboratory of Biotherapy and Cancer Center, West China Hospital, Sichuan University, Chengdu, China. [2]Warshel Institute for Computational Biology, School of Medicine, The Chinese University of Hong Kong, Shenzhen, China. [3]These authors contributed equally: Fei Zhou, Xiaochun He. e-mail: xuemeizhang@scu.edu.cn; lianzhong@scu.edu.cn

https://doi.org/10.1038/s41467-024-55310-x

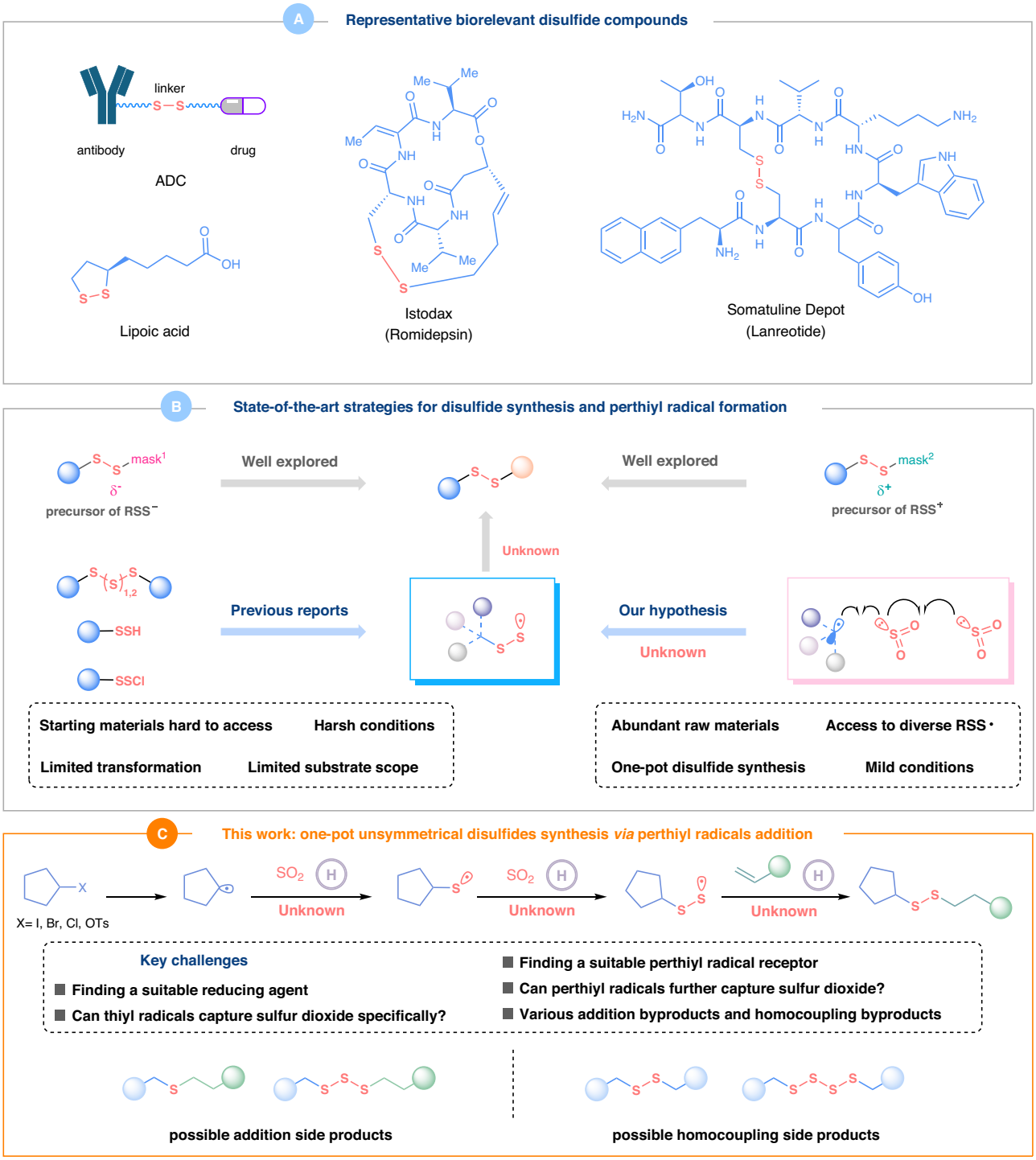

Fig. 1 | Development of a perthiyl radical generation strategy for the synthesis of unsymmetric disulfides. A Representative biorelevant disulfide compounds. **B** Strategies for unsymmetric disulfides construction and perthiyl radical generation. **C** This work: one-pot unsymmetrical disulfides synthesis via perthiyl radicals addition.

the sulfur source to obtain perthiyl radicals for the synthesis of unsymmetric disulfides from easily accessible starting materials in one pot. To achieve this desired reaction, our hypothesis is that a sulfonyl radical can be reduced to a sulfur radical, which can then capture the second SO_2 molecule and undergo subsequent reduction to form the target perthiyl radical (Fig. 1B). Implementing of this protocol presents several challenges: (1) A suitable reducing agent which can effectively reduce sulfonyl radicals to sulfur radicals is in need. (2) The sulfur radicals have to capture SO_2 specifically. (3) Perthiyl radicals are thermodynamically stable and readily form dimers, making the search for a suitable perthiyl radical receptor an intriguing task. (4) The question arises as to whether the perthiyl radicals would continue to capture one more SO_2 molecule. (5) Sulfur radical addition products and perthiyl radical homocoupling products may be produced instead of the desired disulfides.

In this study, perthyl radicals are generated from easily accessible alkyl halides and SO_2, enabling the one-step synthesis of unsymmetric disulfides. This process entails two instances of C–S bond formation and one instance of S–S bond formation (Fig. 1C).

https://doi.org/10.1038/s41467-024-55310-x

Table 1 | Optimization of the reaction conditions[a]

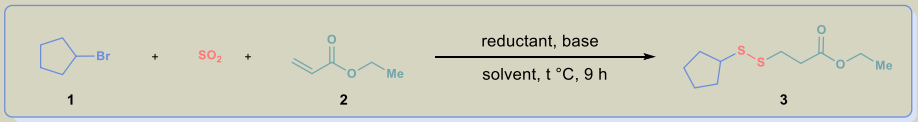

1 2 3

Entry	Deviation from standard conditions	Yield of 3[b]
1	none	72% (72%)[c]
2	without $PhSiH_3$	ND
3	without HCOOLi	ND
4	Et_3SiH instead of $PhSiH_3$	5%
5	PMHS instead of $PhSiH_3$	trace
6	$NaBH_4$ instead of $PhSiH_3$	trace
7	K_2CO_3 instead of HCOOLi	32%
8	DABCO instead of HCOOLi	42%
9	HCOOK instead of HCOOLi	55%
10	S_8 instead of SOgen	49%
11	DABSO instead of SOgen	27%
12	$K_2S_2O_5$ instead of SOgen	ND
13	DMSO instead of DMSO: NMP (1:1)	60%
14	NMP instead of DMSO: NMP (1:1)	43%

ND not detected.
[a]Standard conditions: chamber A, **1** (0.2 mmol, 1.0 equiv), **2** (0.5 mmol, 2.5 equiv), $PhSiH_3$ (0.64 mmol, 3.2 equiv), HCOOLi (0.6 mmol, 3.0 equiv), DMSO (1.0 mL) and NMP (1.0 mL), at 40 °C for 9 h under argon atmosphere. chamber B, SOgen (0.51 mmol), 1-methyl-4-vinylbenzene (0.5 mmol), tetradecane (1.0 mL), at 100 °C for 10 min.
[b]Yields were determined by GC using dodecane as an internal standard.
[c]Isolated yield in parentheses.

Results

Reaction optimization

The disulfide reaction was initially investigated by studying the reaction between the model reactants 1-bromocyclopentane **1**, ethyl acrylate **2** and ex-situ generated SO_2 gas (from SOgen)[36] (Table 1). The optimized conditions were: $PhSiH_3$ (3.2 equiv) as reductant, HCOOLi (3.0 equiv) as the base, a 1:2.5:2.5 ratio of 1-bromocyclopentane to ethyl acrylate to SO_2, 2.0 mL mixture of NMP-DMSO (1:1) as solvent and 40 °C as the reaction temperature. Under these conditions, product **3** was obtained in 72% isolated yield (entry 1, Table 1). The reaction did not occur in the absence of $PhSiH_3$ or HCOOLi (entries 2–3). Substituting $PhSiH_3$ with Et_3SiH as the reductant resulted in a substantial reduction in the product yield (entry 4), while the use of other reductant sources such as PMHS and $NaBH_4$ directly suppressed the reaction (entries 5–6). It was observed that the choice of base had a significant impact on the reaction. Replacing HCOOLi with K_2CO_3, DABCO, and HCOOK led to a dramatic decrease in yields (entries 7–9). In addition, two alternative SO_2 surrogates and S_8 were explored. Using S_8 instead of SO_2 resulted in product yields of 49% (entry 10). The use of DABSO resulted in a significantly reduced yield (entry 11), while the utilization of another inorganic SO_2 surrogate, namely $K_2S_2O_5$ (entry 12), completely hindered the conversion. Furthermore, the choice of solvent also influenced the reaction outcome. The use of DMSO or NMP resulted in product yields of only 60% and 43%, respectively (entries 13–14). Instead, a mixture of 1:1 DMSO and NMP was found to be the optimal solvent for the reaction.

Substrate scopes

With the optimal reaction conditions identified, we proceeded to explore the generality of the reaction. First, the scope with respect to the alkyl bromides was investigated (Fig. 2). We observed that both linear and α-branched primary alkyl bromides could be successfully converted into the corresponding disulfides (**4**-**8**). The reaction exhibited a high chemoselectivity for activating alkyl bromides over alkyl fluorides, as evidenced by the formation of product **9**. In addition, the alkyl bromides bearing remote functional groups, such as benzyl ether and trimethylsilane, were found to be compatible with the reaction conditions (**10,11**). Moreover, alkyl bromides bearing aromatic rings, such as non-substituted and substituted phenyl and naphthyl rings, proved to be suitable substrates in the transformation (**12**-**16**). Notably, we found that heterocycle substituents, such as N-protected pyrrolidines, N-protected piperazine, thiophene, were well-tolerated on the alkyl bromides (**17**-**19**). Additionally, substrates containing unsaturated propargyl and allyl derivatives underwent the conversion smoothly, providing the desired products (**20, 21**). Next, secondary alkyl bromides were tested in the reaction. Apart from the model product **3**, some secondary alkyl bromides with various carbon chain length could lead to the desired products (**22**-**25**). Interestingly, various secondary benzyl bromides were also suitable substrates, successfully providing products **26**-**28**. In addition, two examples of α-carbonyl alkyl bromides went through the transformation and gave the target disulfides (**29, 30**). To our delight, tertiary alkyl bromides with large steric hindrance were also proved amenable for the reaction (**31**-**33**), indicating that this strategy had potential for the construction of hindered unsymmetrical disulfides.

Continuously, a series of alkyl iodides were employed in the reaction in place of the model reactant alkyl bromides (Fig. 3). Pleasingly, disulfide products **4, 7, 11, 12, 23,** and **27** which could be prepared from primary alkyl bromides were also successfully prepared from alkyl iodides. Primary alkyl iodide with longer carbon chain was tolerated in the reaction, providing the target product **34**. Two secondary alkyl iodides also went the reaction smoothly and produced the desired products **23** and **27**. In the same way, alkyl chlorides were used in place of bromide analogs (Fig. 3). Alkyl chlorides containing terminal alkene, terminal alkyne or allyl group could afford the corresponding products **21, 35** and **36** respectively. Some secondary alkyl chlorides were also suitable substrates for this protocol (**23, 26, 27**). It was gratifying that pseudohalides were compatible with the reaction conditions. Various alkyl tosylates could be converted into the corresponding disulfides in 45%-69% yields (Fig. 3). For example, products **4,**

https://doi.org/10.1038/s41467-024-55310-x

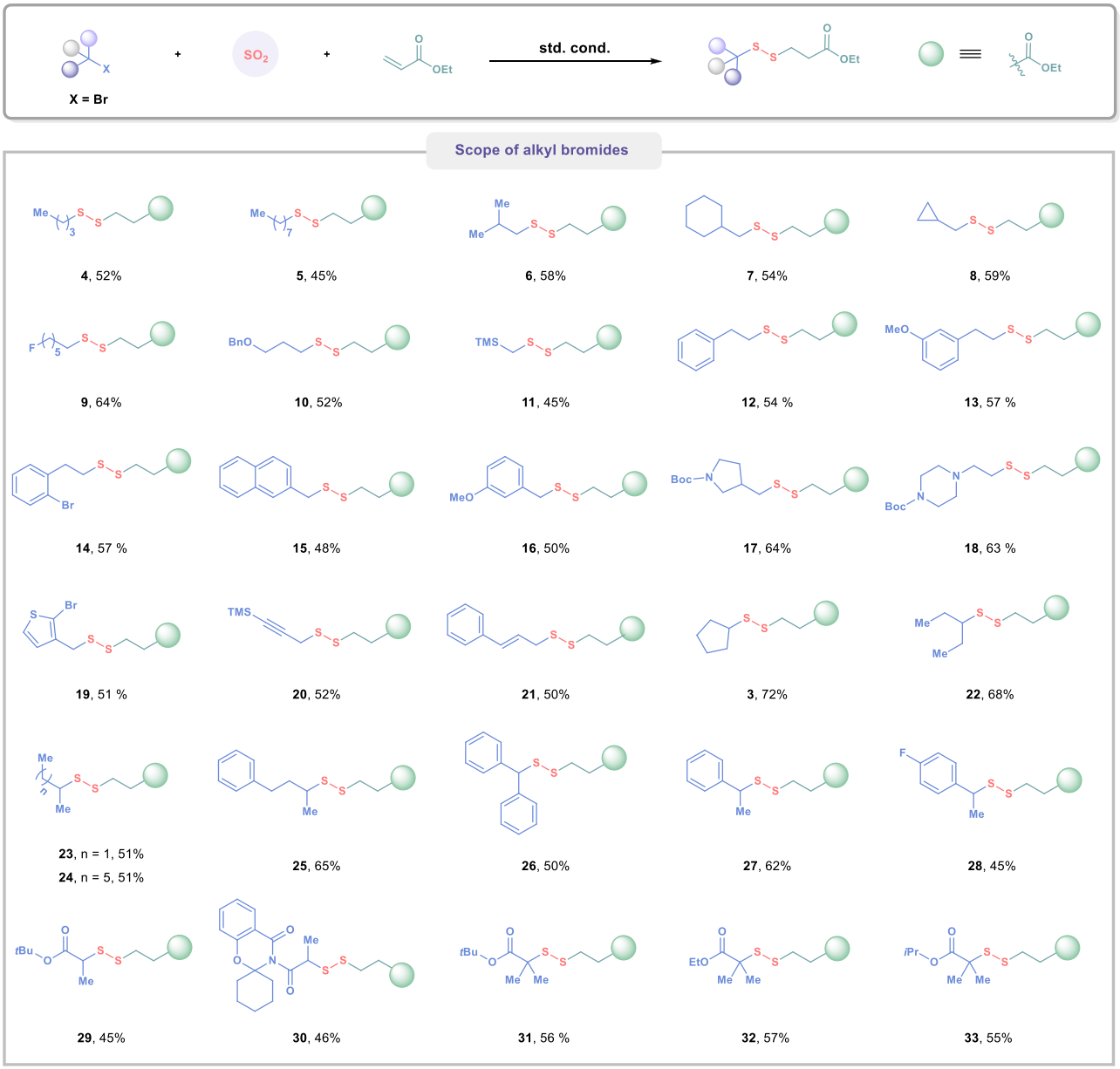

Fig. 2 | Substrate scope of alkyl bromides. Reaction conditions: alkyl bromides (0.2 mmol, 1.0 equiv), *α*, *β*-unsaturated esters (0.5 mmol, 2.5 equiv), SO_2 (0.5 mmol, 2.5 equiv), $PhSiH_3$ (0.64 mmol, 3.2 equiv), HCOOLi (0.6 mmol, 3.0 equiv), DMSO (1.0 mL) and NMP (1.0 mL), at 40 °C for 9 h under argon atmosphere. Isolated yields were reported. std. cond. = standard conditions.

12 were obtained again by using primary alkyl tosylates instead of the primary alkyl bromides. This protocol also had good tolerance for alkyl tosylates containing aromatic rings decorated with various substituents (**37**-**41**). Tosylate substrates containing heterocycles and terminal alkene were also compatible with this transformation (**42**-**44**). Both linear (**45, 25, 22**) and cyclic (**3, 46, 47**) secondary alkyl tosylates successfully underwent the desired transformation.

We next began to investigate the scope of alkene derivatives for the reaction (Fig. 4). *α*, *β*-unsaturated esters (**48**-**56**) were all tolerated under the standard experiment conditions. Interestingly, excellent regioselectivity of the reaction was demonstrated by using vinyl acrylate as a reactant (**55**). To our delight, vinyl pyridine could be used as an effective perthiyl radical acceptor (**57**). *α*-aryl substituted *α*, *β*-unsaturated ester was also proved to be a suitable substrate, providing product **58** in moderate yield. Additionally, *α*, *β*-unsaturated amide could readily participate in the reaction (**59**). Furthermore, we aimed to showcase the practical applications of this strategy by utilizing pharmaceuticals and natural products as reaction substrates for modification purposes. As a results, disulfides derived from Diacetonefructose (**60**), Estrone (**61**), Paroxetine (**62**), L-Menthol (**63**) and DL-*α*-Tocopherol (**64**) were successfully prepared respectively.

Mechanistic investigations

To shed light on the nature of this reaction system, radical trapping experiments were carried out (Fig. 5A). When the reaction was conducted without ethyl acrylate, the TEMPO-carbon radical adduct compound **65** was detected. When TEMPO was added to the standard reaction in which SO_2 was added, the target disulfide **3** was not observed and the S-centered radical was efficiently trapped by TEMPO (**66**). Moreover, when TEMPO was added after 20 min of the reaction, perthiyl radicals and sulfur radicals were generated and trapped, proved by the detection of **66** and **67**. Next, the parallel kinetic isotope effect (KIE) experiments (from initial rate) showed that the k_H/k_D value was 4.43, and the competitive KIE was determined to be $k_H/k_D = 2.57$,

https://doi.org/10.1038/s41467-024-55310-x

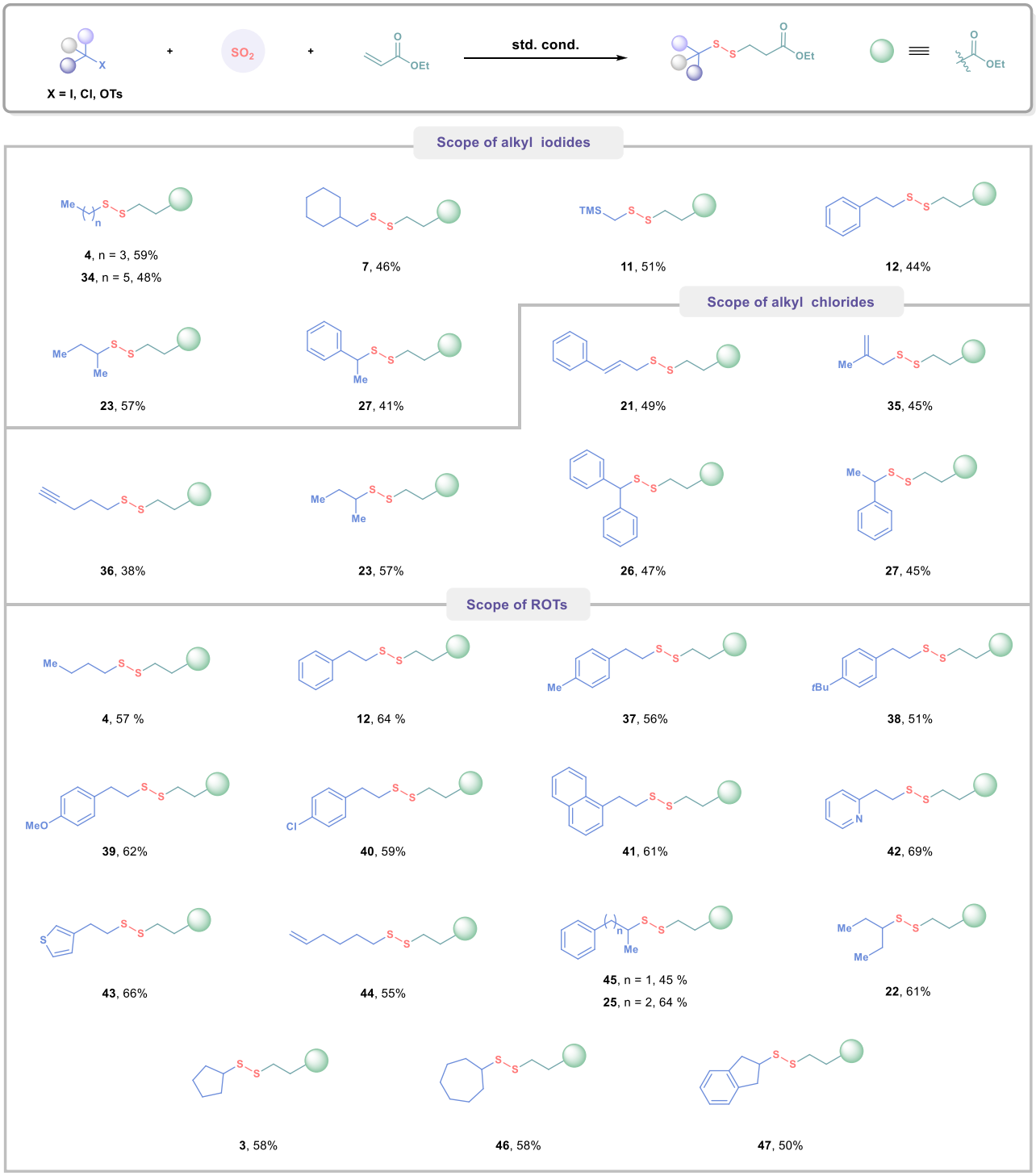

Fig. 3 | Substrate scope of alkyl iodides, alkyl chlorides and alkyl tosylates. Reaction conditions: alkyl electrophile (0.2 mmol, 1.0 equiv), α, β-unsaturated esters (0.5 mmol, 2.5 equiv), SO_2 (0.5 mmol, 2.5 equiv), $PhSiH_3$ (0.64 mmol, 3.2 equiv), HCOOLi (0.6 mmol, 3.0 equiv), DMSO (1.0 mL) and NMP (1.0 mL), at 40 °C for 9 h under argon atmosphere. Isolated yields were reported. std. cond. = standard conditions.

indicating that the protonation step was involved in the turnover-limiting step (Fig. 5B). In the template reaction, we have identified two side products: disulfide compound **68** with a yield of 9% and trisulfide compound **69** with a yield of 5%. Subsequently, we performed a control experiment under standard reaction conditions, excluding the addition of ethyl acrylate. Dimers of disulfides **68**, trisulfides **69**, and tetrasulfides **70** were identified, with yields of 32%, 25%, and 18%, respectively. To gain more insight into the reaction mechanism, symmetrical disulfide **68**, trisulfide **69**, or tetrasulfide **70** was utilized in place of reactant **1** in reactions with reactant **2**, all eventually generating product **3** in yields of 50%, 53%, and 45%, respectively. Additionally, trace amount of thioether **3"** was detected in the reaction between compound **68** and ethyl acrylate. In the template reaction, 1.0 equivalent of SO_2 was used instead of 2.5 equivalents, and as a result, trace amount of thioether product **3"** was detected by GCMS. These results indicate the generation of sulfur radicals and demonstrate that there is an interconversion between the sulfur radicals and compound **68** throughout the reaction process (Fig. 5C).

https://doi.org/10.1038/s41467-024-55310-x

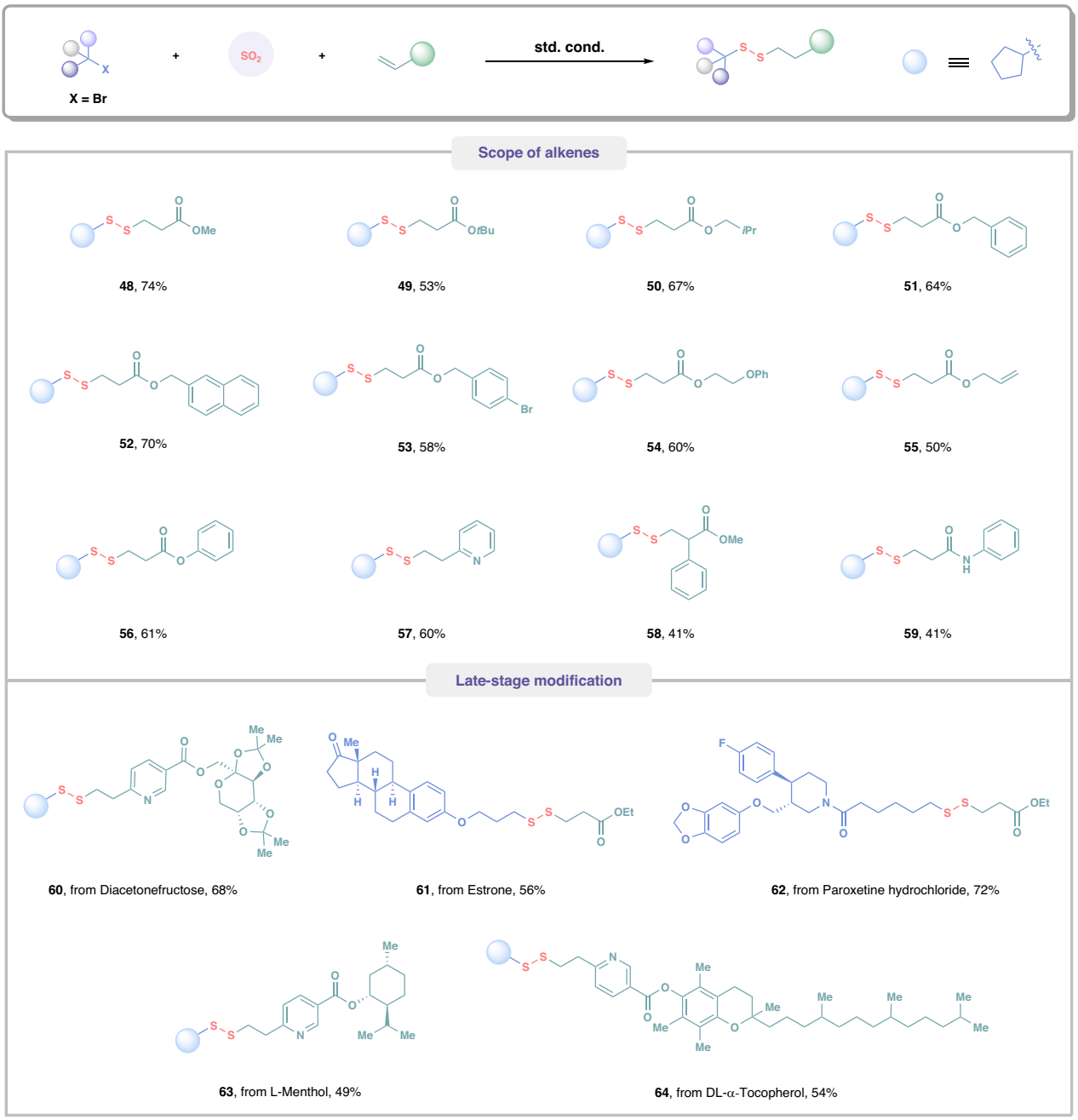

Fig. 4 | Substrate scope of alkenes and coupling with natural products or pharmacologically active molecules. Reaction conditions: alkyl bromides (0.2 mmol, 1.0 equiv), α, β-unsaturated esters (0.5 mmol, 2.5 equiv), SO_2 (0.5 mmol, 2.5 equiv), $PhSiH_3$ (0.64 mmol, 3.2 equiv), HCOOLi (0.6 mmol, 3 equiv), DMSO (1.0 mL) and NMP (1.0 mL), at 40 °C for 9 h under argon atmosphere. Isolated yields were reported. std. cond. = standard conditions.

Proposed mechanism

On the basis of the initial mechanistic studies, a plausible reaction mechanism is proposed herein (Fig. 5D). Initially, the key species **I** may be generated from the interaction between alkyl bromide and a radical initiator which generated from the silane. Secondly, the alkyl radical **I** is trapped by SO_2 to form the alkylsulfonyl radical species **II**, which would undergo fast deoxygenation, giving thiyl radical intermediate **III**, which has an equilibrium with compound **68**. Intermediate **III** could capture an additional molecule of SO_2, and then undergoes the same deoxygenation process to yield perthiyl radical **IV**. **IV** may either couple with **III** or undergo homo-coupling to form compounds **69** and **70**, respectively. This process is reversible. Then, perthiyl radical adds to **2** and generates **V** which then undergoes HAT with $PhSiH_3$ to produce the disulfuration product **3**.

DFT studies

To gain more in-depth insights into the reaction mechanism, density functional theory (DFT) calculations were conducted (Fig. 6). Silicon radical formation through $PhSiH_3$ is the initiation step[67–69]. First of all, we found that the base additive ($HCOO^-$) enables a much more facile reaction pathway. Its binding with $PhSiH_2$ radical is exergonic by -2.8 kcal/mol, resulting in a new radical intermediate $PhSiH_2$-$HCOO^{\bullet-}$, which is a quite strong reductant (E^{ox} = −2.51 V versus NHE). In addition, the silane-formate complex, $PhSiH_3$-$HCOO^-$, exhibits a significantly elongated Si–H bond (1.57 angstrom, versus 1.48 angstrom in $PhSiH_3$),

https://doi.org/10.1038/s41467-024-55310-x

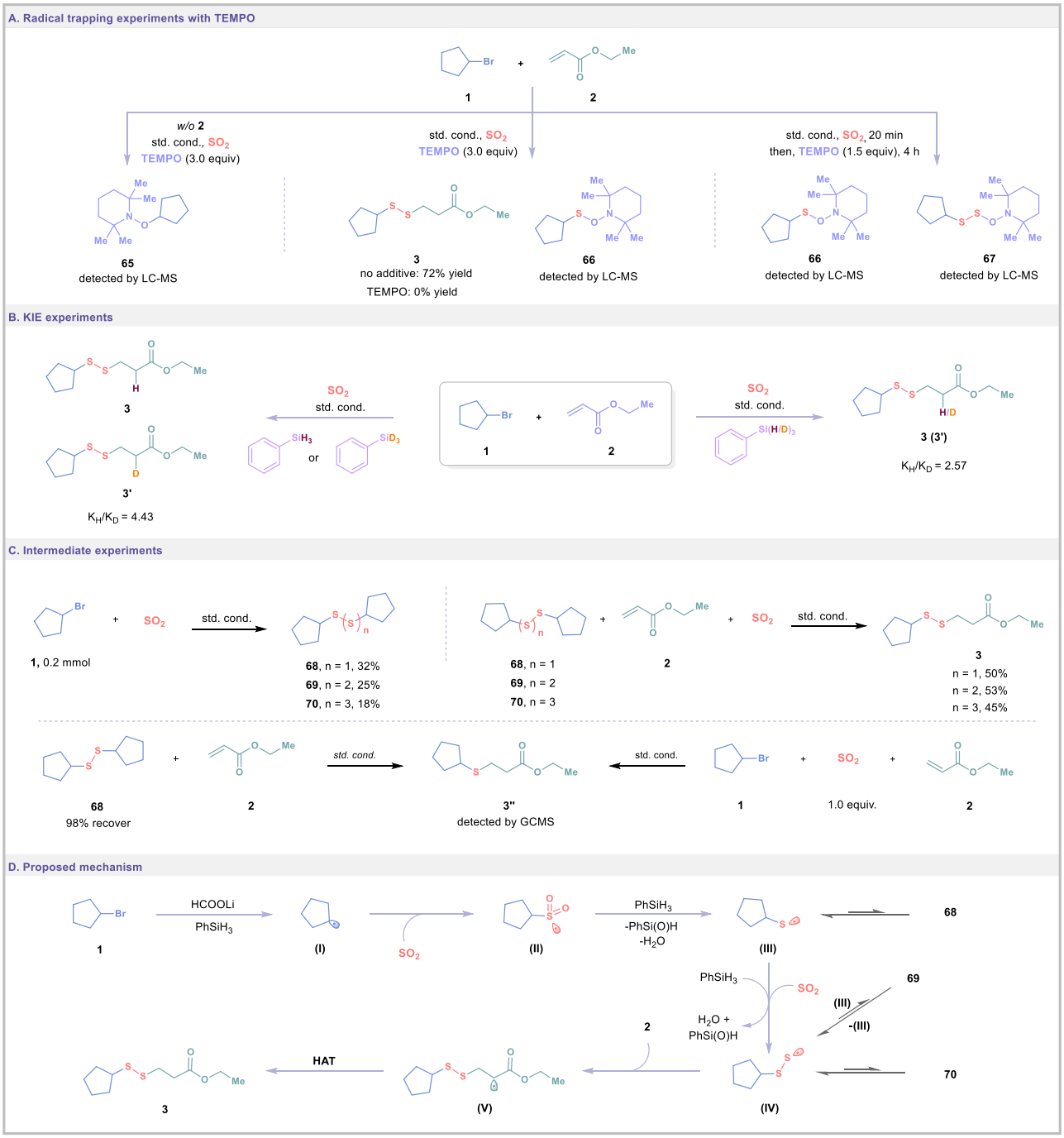

Fig. 5 | Key mechanistic findings. A Radical-trapping experiments with TEMPO; **B** KIE experiments; **C** Intermediate experiments; **D** Proposed mechanism. std. cond. = standard conditions.

indicating that it may act as a superstrong hydrogen donor. Then, the halogen-atom transfer (XAT) process between **1** and $PhSiH_2$-$HCOO^{\bullet-}$ resulting in the formation of alkyl radical (**INT1**) is determined to have a free energy barrier of 14.5 kcal/mol (**TS1**). Following that, SO_2 is rapidly trapped by **INT1** without encountering any energy barrier (Supplementary Fig. 8). We have calculated the barrier for the addition of **INT2** to alkene, which is 16.6 kcal/mol. As the reduction of **INT2** is barrierless, the addition will not form a competitive side product pathway. The hydrogen transfer from $PhSiH_3$-$HCOO^-$ to **INT2** is barrierless, resulting in the formation of **INT3** and $PhSiH_2$-$HCOO^{\bullet-}$. Then they immediately undergo a single electron transfer event, and the so-generated radical anion **INT4** and $PhSiH_2OOCH$ rapidly re-associate to afford **INT4'**. Then, the **INT4'** undergoes deoxygenation through the cleavage of the S–OH bond, hydrogen abstraction, and sequential radical elimination to produce sulfur radical (**INT6**) and poly(-phenylsiloxanes), which may exist in linear or cyclic (**INT5**, detected by HRMS) forms. Its free energy profile has been explored in Supplementary Fig. 9. Next, we have calculated the barrier for the addition of **INT6** to alkene, which is 13.8 kcal/mol, as well as determined that the homocoupling of **INT6** occurs barrierlessly. However, as shown in the energy profile, once **INT6** is transformed into **INT7**, it is barrierlessly reduced, furthermore, the energy barrier required for the irreversible transformation from **INT6** to **INT7** is 11.2 kcal/mol. As a result, the thioether product will not form. Considering that compound **68** may represent an important resting state during the reaction, we further investigated the relevant mechanisms of the transformation of

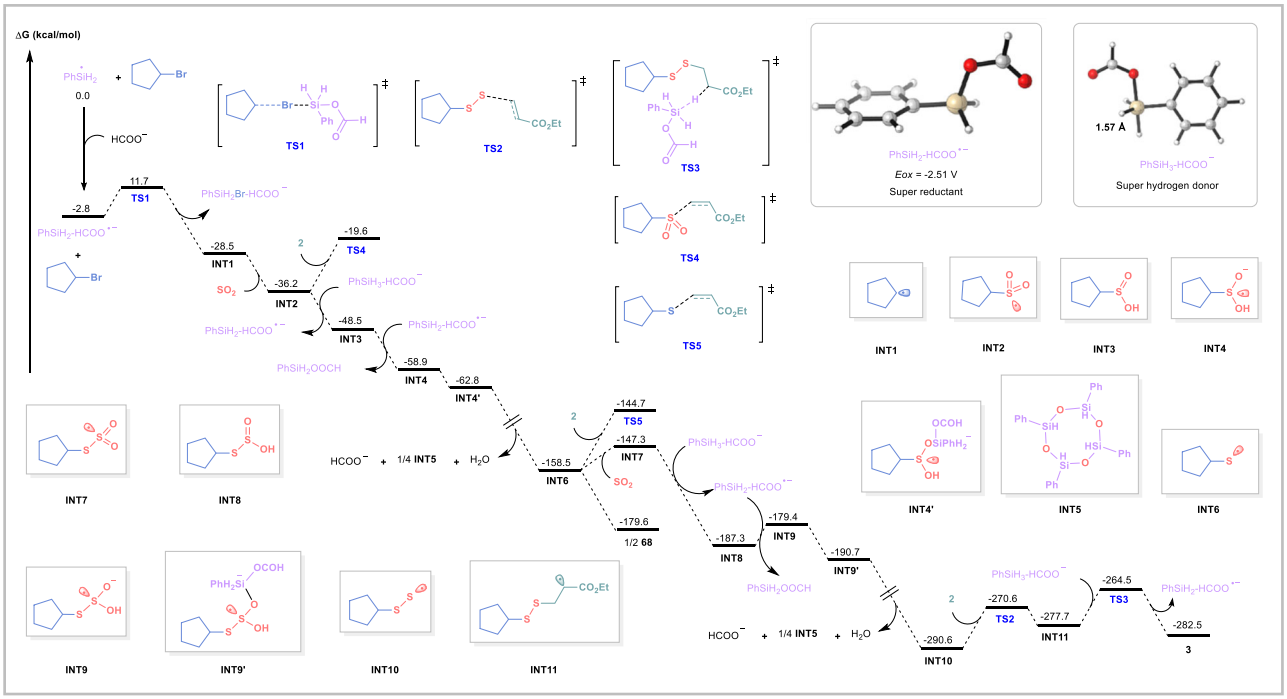

Fig. 6 | The free energy profile for the alkene hydro-disulfuration reactions. All molecular geometries were optimized at the M06-2X/6-31 + G(d) level of theory using SMD model to account for solvation energies in DMSO.

compound **68**, as shown in Supplementary Fig. 10. Subsequently, **INT7** is reduced barrierlessly by $PhSiH_3$-$HCOO^-$, after which **INT8** undergoes a single-electron transfer with a free energy barrier of 7.9 kcal/mol. And then, **INT9** and $PhSiH_2OOCH$ rapidly re-associate to afford **INT9'**. Next, **INT9'** undergoing deoxygenation is similar to that of transforming **INT4'** into **INT6**, resulting in the formation of perthiyl radical (**INT10**), as shown in Supplementary Fig. 9. We have found that the association of **INT10** with the third equivalent of SO_2 unable to give any minimum on the potential energy surface, and thus further combination with SO_2 is unrealistic (Supplementary Fig. 11). The perthiyl radical has the ability to undergo addition to ethyl acrylate (**2**), resulting in the formation of a carbon-centered radical (**INT11**) with a free energy barrier of 20.0 kcal/mol (**TS2**). Subsequently, this newly formed radical abstracts a hydrogen atom from $PhSiH_3$-$HCOO^-$ through transition state **TS3** with an activation free energy of 26.1 kcal/mol to yield the desired product **3** and $PhSiH_2$-$HCOO^{\bullet-}$ which participates in the propagating chain process. The overall barrier is 26.1 kcal/mol, as determined by the hydrogen abstraction of the radical **INT11** via the transition state **TS3**. Overall, the pathway calculated by DFT is consistent with the assumption described in Fig. 5D.

In summary, we have developed a unified protocol for hydro-disulfuration of alkenes with alkyl electrophiles under mild conditions. This reaction uses readily abundant alkyl electrophiles and alkenes as starting materials, providing straightforward access to unsymmetrical disulfides with excellent functional group tolerance. It is demonstrated as an effective example of the synthesis of unsymmetrical disulfides by using SO_2 as a divalent sulfur source. Phenylsilane serves both as the radical initiator and reductant. This research provides a convenient method for synthesis of unsymmetrical disulfides which are challenging to access. Further investigations will focus on expanding the perthiyl radical acceptor scope and finding widespread application for this disulfuration strategy.

Methods

General procedure for the synthesis of compounds **3-64:** In an argon fulfilled glovebox, perbromothiophene 1,1-dioxide (219.8 mg, 0.51 mmol, 2.5 equiv), tetradecane (1.0 mL), were added into chamber B with a magnetic stirring bar, followed by addition of 1-methyl-4-vinylbenzene (59.3 mg, 0.5 mmol, 2.5 equiv). HCOOLi (0.6 mmol, 31.2 mg), alkyl electrophiles (-Cl/-Br/-I/-OTs) (0.2 mmol) and alkenes (0.5 mmol) were added into chamber A, then anhydrous NMP (1.0 mL) and DMSO (1.0 mL) was added into chamber A. Then, $PhSiH_3$ (0.64 mmol, 79 μL) was added into chamber A by microsyringe. The two-chamber was sealed and removed out of the glovebox. The chamber B was allowed to stir at 100 °C using heating mantle with 600 rpm stirring speed for 10 min (chamber A was not allowed to stir). After then, the chamber A was allowed to stir at 40 °C using heating mantle with 300 rpm stirring speed for 9 h. Upon completion, the reaction was quenched with water (30 mL) and extracted with EA (30 mL). The extract was washed by brine (15 mL) and dried over anhydrous Na_2SO_4. After filtering, the filtrate was concentrated, and the residue was purified by flash silica gel column chromatography using petroleum ether/ethyl acetate as eluent to afford pure products **3-64**.

Data availability

The authors declare that all data generated or analyzed during this study are included in this article and Supplementary Information. The energetics and Cartesian coordinates for all species are presented in the Supplementary Data 1. Data are also available from the corresponding author upon request.

References

1. Lee, M. H. et al. Disulfide-cleavage-triggered chemosensors and their biological applications. *Chem. Rev.* **113**, 5071–5109 (2013).
2. Silva, F. et al. Short total synthesis of ajoene. *Angew. Chem. Int. Ed.* **57**, 12290–12293 (2018).
3. Góngora-Benítez, M., Tulla-Puche, J. & Albericio, F. Multifaceted roles of disulfide bonds. peptides as therapeutics. *Chem. Rev.* **114**, 901–926 (2014).
4. Beck, A., Goetsch, L., Dumontet, C. & Corvaïa, N. Strategies and challenges for the next generation of antibody–drug conjugates. *Nat. Rev. Drug Discov.* **16**, 315–337 (2017).

5. Zhao, B. & Burgess, K. TrkC-targeted kinase inhibitors and PROTACs. *Mol. Pharm.* **16**, 4313–4318 (2019).
6. Naderi, N., Darmishonnejad, Z., Tavalaee, M. & Nasr-Esfahani, M. H. The effect of alpha-lipoic acid on sperm functions in rodent models for male infertility: a systematic review. *Life Sci.* **323**, 121383 (2023).
7. Yang, L. P. H. Romidepsin. *Drugs* **71**, 1469–1480 (2011).
8. Salvia, L. A. et al. Targeting neuroendocrine tumors with octreotide and lanreotide: Key points for clinical practice from NET specialists. *Cancer Treat. Rev.* **117**, 102560 (2023).
9. Xiao, X., Feng, M. & Jiang, X. New design of a disulfurating reagent: facile and straightforward pathway to unsymmetrical disulfanes by copper-catalyzed oxidative cross-coupling. *Angew. Chem. Int. Ed.* **55**, 14121–14125 (2016).
10. Xiao, X., Xue, J. & Jiang, X. Polysulfurating reagent design for unsymmetrical polysulfide construction. *Nat. Commun.* **9**, 2191 (2018).
11. Xue, J. & Jiang, X. Unsymmetrical polysulfidation *via* designed bilateral disulfurating reagents. *Nat. Commun.* **11**, 4170 (2020).
12. Qi, J., Wei, F., Huang, S., Tung, C.-H. & Xu, Z. Copper(I)-catalyzed asymmetric interrupted Kinugasa reaction: synthesis of α-thio-functional chiral β-lactams. *Angew. Chem. Int. Ed.* **60**, 4561–4565 (2021).
13. Zhang, Q., Li, Y., Zhang, L. & Luo, S. Catalytic asymmetric disulfuration by a chiral bulky three-component Lewis acid-base. *Angew. Chem. Int. Ed.* **60**, 10971–10976 (2021).
14. Chen, X., Shao, W. & Deng, G.-J. Nickel-catalyzed deoxygenative disulfuration of alcohols to access unsymmetrical disulfides. *ACS Catal.* **14**, 6451–6461 (2024).
15. Chen, S. et al. Sandmeyer-type reductive disulfuration of anilines. *Org. Lett.* **23**, 7428–7433 (2021).
16. Bai, Z. et al. Synthesis of *N*-acyl sulfenamides *via* copper catalysis and their use as S-sulfenylating reagents of thiols. *Nat. Commun.* **13**, 6445 (2022).
17. Zou, J. et al. Phthalimide-carried disulfur transfer to synthesize unsymmetrical disulfanes *via* copper catalysis. *ACS Catal.* **9**, 11426–11430 (2019).
18. Ren, X. et al. Access to polysulfides through photocatalyzed dithiosulfonylation. *Angew. Chem. Int. Ed.* **62**, e202302199 (2023).
19. Tian, Q. & Li, Y. Design of a bilateral disulfurating reagent for unsymmetrical polysulfidation. *Angew. Chem. Int. Ed.* **62**, e202302861 (2023).
20. Asanuma, H., Kanemoto, K., Watanabe, T. & Fukuzawa, S.-I. *N*-(Morpholine-4-dithio)phthalimide: a shelf-stable, bilateral platform molecule enabling access to diverse unsymmetrical disulfides. *Angew. Chem. Int. Ed.* **62**, e202219156 (2023).
21. Yu, Q., Zhang, X. & Jiang, X. Bilateral unsymmetrical disulfurating reagent design for polysulfide construction. *Angew. Chem. Int. Ed.* **63**, e202408158 (2024).
22. Zhang, J. & Studer, A. Decatungstate-catalyzed radical disulfuration through direct C-H functionalization for the preparation of unsymmetrical disulfides. *Nat. Commun.* **13**, 3886 (2022).
23. Wu, Z. & Pratt, D. A. Radical substitution provides a unique route to disulfides. *J. Am. Chem. Soc.* **142**, 10284–10290 (2020).
24. Huang, H., Wu, Z. & Pratt, D. A. Photocatalytic C–S bond formation using *N*-thiophthalimide and *N*-perthiophthalimide derivatives. *ACS Catal.* **13**, 13912–13919 (2023).
25. Wu, Z. & Pratt, D. A. A divergent strategy for site-selective radical disulfuration of carboxylic acids with trisulfide-1,1-dioxides. *Angew. Chem. Int. Ed.* **60**, 15598–15605 (2021).
26. Burkey, T. J. et al. The *tert*-butylperthiyl radical. *J. Org. Chem.* **50**, 4966–4967 (1985).
27. Kende, I., Pickering, T. L. & Tobolsky, A. V. The dissociation energy of the tetrasulfide linkage. *J. Am. Chem. Soc.* **87**, 5582–5586 (1965).
28. Benson, S. W. Thermochemistry and kinetics of sulfur-containing molecules and radicals. *Chem. Rev.* **78**, 23–35 (1978).
29. Hawari, J. A., Griller, D. & Lossing, F. P. Thermochemistry of perthiyl radicals. *J. Am. Chem. Soc.* **108**, 3273–3275 (1986).
30. Chauvin, J.-P. R., Haidasz, E. A., Griesser, M. & Pratt, D. A. Polysulfide-1-oxides react with peroxyl radicals as quickly as hindered phenolic antioxidants and do so by a surprising concerted homolytic substitution. *Chem. Sci.* **7**, 6347–6356 (2016).
31. Everett, S. A., Schoeneich, C., Stewart, J. H. & Asmus, K. D. Perthiyl radicals, trisulfide radical ions, and sulfate formation: a combined photolysis and radiolysis study on redox processes with organic di- and trisulfides. *J. Phys. Chem. A* **96**, 306–314 (1992).
32. Wu, Z., Back, T. G., Ahmad, R., Yamdagni, R. & Armstrong, D. A. Mechanism of reduction of bis(2-hydroxyethyl) trisulfide by eaq^- and.bul.CO-2. Spectrum and scavenging of RSS.bul. radicals. *J. Phys. Chem. C* **86**, 4417–4422 (1982).
33. Lindahl, S. & Xian, M. Recent development of polysulfides: chemistry and biological applications. *Curr. Opin. Chem. Biol.* **75**, 102325–102331 (2023).
34. Everett, S. A., Folkes, L. K., Wardman, P. & Asmus, K. D. Free-radical repair by a novel perthiol: reversible hydrogen transfer and perthiyl radical formation. *Free Radic. Res.* **20**, 387–400 (1994).
35. Terryn, H., Tilquin, B. & Houée-Levin, C. Formation of perthiyl free radicals in irradiated glutathione. *Res. Chem. Intermed.* **31**, 727–736 (2005).
36. Jia, X., Kramer, S., Skrydstrup, T. & Lian, Z. Design and applications of a SO_2 surrogate in palladium-catalyzed direct aminosulfonylation between aryl iodides and amines. *Angew. Chem. Int. Ed.* **60**, 7353–7359 (2021).
37. Chen, L. et al. Enantioselective four-component arylsulfonylcyanation of vinylarenes *via* the insertion of SO_2 enabled by SOgen as SO_2 surrogate. *ACS Catal.* **12**, 10764–10770 (2022).
38. Qiu, G., Lai, L., Cheng, J. & Wu, J. Recent advances in the sulfonylation of alkenes with the insertion of sulfur dioxide *via* radical reactions. *Chem. Commun.* **54**, 10405–10414 (2018).
39. Ye, S., Qiu, G. & Wu, J. Inorganic sulfites as the sulfur dioxide surrogates in sulfonylation reactions. *Chem. Commun.* **55**, 1013–1019 (2019).
40. Zhang, J., Wang, P., Li, Y. & Wu, J. Asymmetric sulfonylation with sulfur dioxide surrogates: a new access to enantiomerically enriched sulfones. *Chem. Commun.* **59**, 3821–3826 (2023).
41. Zeng, D., Wang, M., Deng, W. & Jiang, X. The same oxygenation-state introduction of hypervalent sulfur under transition-metal-free conditions. *Org. Chem. Front.* **7**, 3956–3966 (2020).
42. Wang, M. & Jiang, X. The Same oxidation-state introduction of hypervalent sulfur *via* transition-metal catalysis. *Chem. Rec.* **21**, 3338–3355 (2021).
43. Emmett, E. J. & Willis, M. C. The development and application of sulfur dioxide surrogates in synthetic organic chemistry. *Asian J. Org. Chem.* **4**, 602–611 (2015).
44. Blum, S. P., Hofman, K., Manolikakes, G. & Waldvogel, S. R. Advances in photochemical and electrochemical incorporation of sulfur dioxide for the synthesis of value-added compounds. *Chem. Commun.* **57**, 8236–8249 (2021).
45. Chen, G. & Lian, Z. Multicomponent reactions based on SO_2 surrogates: recent advances. *Eur. J. Org. Chem.* **26**, e202300217 (2023).
46. Chen, Y., Murray, P. R. D., Davies, A. T. & Willis, M. C. Direct copper-catalyzed three-component synthesis of sulfonamides. *J. Am. Chem. Soc.* **140**, 8781–8787 (2018).
47. Huang, J. et al. Accessing chiral sulfones bearing quaternary carbon stereocenters via photoinduced radical sulfur dioxide insertion and Truce–Smiles rearrangement. *Nat. Commun.* **13**, 7081 (2022).
48. Meng, Y., Wang, M. & Jiang, X. Multicomponent reductive cross-coupling of an inorganic sulfur dioxide surrogate: straightforward construction of diversely functionalized sulfones. *Angew. Chem. Int. Ed.* **59**, 1346–1353 (2020).

49. Li, H. et al. Synthesis of multifluoromethylated γ-sultines by a photoinduced radical addition–polar cyclization. *Angew. Chem. Int. Ed.* **62**, e202300159 (2023).
50. Lou, T. S.-B. et al. Chemoselective nickel electrocatalytic sulfinylation of aryl halides with SO_2. *Angew. Chem. Int. Ed.* **61**, e202208080 (2022).
51. Pedersen, P. S., Blakemore, D. C., Chinigo, G. M., Knauber, T. & MacMillan, D. W. C. One-pot synthesis of sulfonamides from unactivated acids and amines *via* aromatic decarboxylative halosulfonylation. *J. Am. Chem. Soc.* **145**, 21189–21196 (2023).
52. Zhao, F. & Wu, X. Sulfonylation of bismuth reagents with sulfinates or SO_2 through Bi^{III}/Bi^{V} intermediates. *Organometallics* **40**, 2400–2404 (2021).
53. Hethcox, J. C. et al. Nickel-catalyzed sulfonylation of aryl bromides enabled by potassium metabisulfite as a uniquely effective SO_2 surrogate. *Angew. Chem. Int. Ed.* **62**, e202217623 (2023).
54. Hou, X., Liu, H. & Huang, H. Iron-catalyzed fluoroalkylative alkylsulfonylation of alkenes *via* radical-anion relay. *Nat. Commun.* **15**, 1480 (2024).
55. Qu, S., Li, X., Li, X. & Wang, L. Copper-catalyzed chemoselective (amino)fluorosulfonylation of hydrocarbons *via* intramolecular fluorine-atom transfer. *ACS Catal.* **14**, 4318–4328 (2024).
56. Chen, Z. et al. Iron-mediated cyanoalkylsulfonylation/arylation of active alkenes with cycloketone oxime derivatives *via* sulfur dioxide insertion. *Adv. Synth. Catal.* **362**, 3004–3010 (2020).
57. Zhou, N. et al. Copper-catalyzed multicomponent oxysulfonylation of alkenes with cyclobutanone oxime esters and hydroxamic acids *via* the insertion of sulfur dioxide. *Adv. Synth. Catal.* **364**, 4020–4025 (2022).
58. Yang, Y., Xiao, F., Lin, J. & Xiao, J. The shuttle of sulfur dioxide: iridium/copper-cocatalyzed trifluoromethylfluorosulfonylation of alkenes. *Adv. Synth. Catal.* **365**, 301–306 (2023).
59. Zhang, M. et al. Direct synthesis of sulfonamides *via* synergetic photoredox and copper catalysis. *ACS Catal.* **13**, 11580–11588 (2023).
60. Zhang, H. et al. Photocatalytic fluorosulfonylation of aliphatic carboxylic acid NHPI esters. *Org. Chem. Front.* **9**, 4854–4860 (2022).
61. Sun, Y., Li, C., Xi, J., Wei, Z. & Liao, W. Electrochemical tandem cyclization to access sulfonylated fused sultams *via* SO_2 insertion with sodium metabisulfite. *Org. Chem. Front.* **10**, 705–711 (2023).
62. Liang, X. et al. Visible-light-driven electron donor–acceptor complex induced sulfonylation of diazonium salts with sulfinates. *Green. Chem.* **23**, 8865–8870 (2021).
63. Hofman, K., Liu, N. & Manolikakes, G. Radicals and sulfur dioxide: a versatile combination for the construction of sulfonyl-containing molecules. *Chem. Eur. J.* **24**, 11852–11863 (2018).
64. Chen, Z., Liu, N., Bolte, M., Ren, H. & Manolikakes, G. Visible-light mediated 3-component synthesis of sulfonylated coumarins from sulfur dioxide. *Green. Chem.* **20**, 3059–3070 (2018).
65. Liu, Y. et al. Visible-light promoted one-pot synthesis of sulfonated spiro [4,5] trienones from propiolamides, anilines and sulfur dioxide under transition metal-free conditions. *Chem. Commun.* **55**, 12212–12215 (2019).
66. Zhu, H., Shen, Y., Wen, D., Le, Z. & Tu, T. Selective synthesis of ortho-substituted diarylsulfones by using NHC-Au catalysts under mild conditions. *Org. Lett.* **21**, 974–979 (2019).
67. Toutov, A. A. et al. Silylation of C–H bonds in aromatic heterocycles by an earth-abundant metal catalyst. *Nature* **518**, 80–84 (2015).
68. Liu, W. et al. Potassium *tert*-butoxide-catalyzed dehydrogenative C–H silylation of heteroaromatics: a combined experimental and computational mechanistic study. *J. Am. Chem. Soc.* **139**, 6867–6879 (2017).
69. Zhao, S. & Mankad, N. P. Cu-catalyzed hydroxymethylation of unactivated alkyl iodides with CO to provide one-carbon-extended alcohols. *Angew. Chem. Int. Ed.* **57**, 5867–5870 (2018).

Acknowledgements

This work is supported by National Natural Science Foundation of China (22301192), Sichuan Science and Technology Program (2024NSFSC1124), West China Hospital 135 project (ZYYC23017) and Postdoctor Research Fund of West China Hospital, Sichuan University (2024HXBH027). The authors would like to thank Shiyanjia Lab (www.shiyanjia.com) for the support of DFT calculation.

Author contributions

Z.L. and X.Z. conceived the idea and led the project. F.Z., X.H., and M.Z. designed, conducted, and analyzed the experiments. X.H., F.Z., and X.Z. wrote the paper and prepared the Supplementary Information. N.L. interpreted the DFT data. Q.W. assisted in collecting new compounds.

Competing interests

The authors declare no competing interests.

Additional information

Supplementary information The online version contains supplementary material available at https://doi.org/10.1038/s41467-024-55310-x.

Correspondence and requests for materials should be addressed to Xuemei Zhang or Zhong Lian.

Peer review information *Nature Communications* thanks Zhiming Li, Zhen Wang, and Ke Yang for their contribution to the peer review of this work. A peer review file is available.